Corrosion of ruthenium dioxide based cathodes in alkaline medium caused by reverse currents

Susanne Holmin, Lars-Åke Näslund, Arni Sigurdur Ingason, Johanna Rosén and Erik Zimmerman

Original Publication:

Susanne Holmin, Lars-Åke Näslund, Arni Sigurdur Ingason, Johanna Rosén and Erik Zimmerman, Corrosion of ruthenium dioxide based cathodes in alkaline medium caused by reverse currents, 2014, Electrochimica Acta, (146), 30-36.
http://dx.doi.org/10.1016/j.electacta.2014.09.024

Corrosion of ruthenium dioxide based cathodes in alkaline medium caused by reverse currents

Susanne Holmin[a,b,*] Lars-Åke Näslund,[c] Árni S. Ingason,[c] Johanna Rosen,[c] and Erik Zimmerman[a]

[a]Permascand AB, SE-840 10 Ljungaverk, Sweden

[b]Department of Natural Sciences, Mid-Sweden University, SE 870 10 Sundsvall, Sweden

[c]Materials Design, Thin Film Physics Division, Department of Physics, Chemistry, and Biology (IFM), Linköping University, SE-58183 Linköping, Sweden

Keywords: Hydrogen evolution, RuO_2 coatings, Phase transformation, Polarity inversion, Corrosion.

Abstract

A reverse current obtained during power shutdowns in industrial processes, such as chlor-alkali production or alkaline water electrolysis, is deleterious for hydrogen evolving ruthenium dioxide (RuO_2) based cathodes. It has been observed that RuO_2 coatings after a power shutdown, necessary for e.g. maintenance, are severely damaged unless polarization rectifiers are employed. In this work we show why these types of cathodes are sensitive to reverse currents, i.e. anodic currents, after hydrogen evolution. RuO_2 coatings deposited on nickel substrates were subjected to different electrochemical treatments such as hydrogen evolution, oxygen evolution, or reverse currents in 8 M NaOH at 90 °C. Polarity inversion was introduced after hydrogen evolution to simulate the effect of reverse currents. Because of chemical interaction with hydrogen, a significant amount of the RuO_2 coating was transformed into hydroxylated species during cathodic polarization. Our study shows that these hydroxylated phases are highly sensitive to electrochemical corrosion during anodic polarization after extended hydrogen evolution.

*Corresponding author. Phone: +46 691 355 17; fax: +46 691 330 40.
E-mail address: susanne.holmin@permascand.com

1. Introduction

Ruthenium dioxide (RuO_2) or mixtures of RuO_2 and other metal oxides (TiO_2, IrO_2 etc.), deposited on a titanium (Ti) support, have successfully been used as catalytic and durable coatings for decades in different industrial processes such as chlorine or oxygen gas production. These types of electrodes are often referred to as dimensionally stable anodes (DSA®). RuO_2-based coatings have also found practical applications as a catalyst for hydrogen evolution in chlor-alkali production and alkaline water electrolysis [1]. RuO_2 is then usually deposited on nickel (Ni) substrates because of higher corrosion resistance of Ni, compare to e.g. Ti, in highly concentrated alkaline electrolyte at elevated temperatures.

The most challenging drawback for RuO_2-based cathodes is not activity or duration for hydrogen evolution but reverse currents at power shutdowns. For example, when the chlor-alkali process is interrupted, e.g. for maintenance, a reverse current will flow in the electrochemical cell caused by the change in equilibrium, i.e. hypochlorite and other active chlorine species close to the anode surface starts to reduce. As a consequence the RuO_2-based coating on the cathode starts to degrade, which is suggested being caused by oxidation [1-3]. By introducing polarization rectifiers, the effect of reverse currents can be minimized. A cathodic potential is then applied large enough to protect the RuO_2 catalyst from anodic dissolution during a power shutdown [2].

Although several authors have reported loss of catalyst material as an effect of reverse currents [3-6], the long-term stability of RuO_2-based coatings has not been well studied. In the previous studies reverse current was introduced by polarity inversion, i.e. repetitive cycling of the current or potential between the hydrogen and oxygen evolution reaction or by applying an anodic current after extensive hydrogen evolution. Furthermore, different investigations have shown substantial changes in RuO_2 and other mixed oxides after hydrogen evolution. For example, increased voltammetric charge and activation of the catalyst was found with cyclic voltammetry [7-9]. It was suggested that wetting of active sites or hydroxylation of RuO_2 caused the activation process. Studies with X-ray diffraction (XRD) showed an expansion of the RuO_2 crystal lattice caused by hydrogen absorption into the rutile structure while exposed to hydrogen evolution in acidic medium [10]. In addition, other XRD studies have found irreversible decrease and shift of the rutile diffraction peaks for RuO_2 exposed to an alkaline electrolyte [3,11]. Roughening of the electrode surface area caused by strong

hydrogen evolution has also been reported from studies using atomic force microscopy [12] and scanning electron microscopy [13]. All of these studies indicate that RuO_2 is unstable during hydrogen evolution.

According to thermodynamics, RuO_2 exposed to an alkaline electrolyte suggests being reduced to metallic ruthenium during hydrogen evolution [14,15], however, several authors have in the past used X-ray photoelectron spectroscopy (XPS) with the conclusion that metallic ruthenium does not form [8,16,17]. In contradiction to earlier conclusions, we have in a recent work showed that metallic ruthenium, in fact, is formed during hydrogen evolution in an alkaline electrolyte and at high current density [18]. The study further shows that the RuO_2 coating, prior to metallic Ru formation, is subjected to a transformation into ruthenium oxyhydroxide ($RuO(OH)_2$). Earlier, authors have suggested that RuO_2 is partly reduced through hydration or hydroxylation during hydrogen evolution [3,9,11,16], although never studied in detail. Our detailed material characterization support hydroxylation, however not through a reduction process but instead via a nonelectrochemical process induced by hydrogen incorporation into the RuO_2 rutile crystal structure [18].

The influence of reverse currents on the stability of the formed $RuO(OH)_2$ has, to our best knowledge, never been studied in detail before. Therefore, we have applied several material characterization techniques, such as scanning electron microscopy (SEM), X-ray diffraction (XRD), and X-ray fluorescence (XRF), to study the corrosion behavior of RuO_2-based coatings in a strong alkaline environment after different electrochemical treatments. The sample treatments include the hydrogen evolution reaction (HER), the oxygen evolution reaction (OER), and in addition a sequence of alternating HER and OER for the effect of reverse currents. Understanding the corrosion mechanism for RuO_2-based cathodes during working conditions, such as hydrogen evolution in alkaline environment, is important before further improvements of the activity and stability of said coatings can be developed.

2. Experimental section

2.1. Electrode preparation

The spin coating technique was implemented to assure that reproducible samples were obtained [19,20]. Nickel disks (Ni-201) with a diameter of 25 mm and thickness of 1 mm were used as substrates. Prior to coating, the disks were blasted with Al_2O_3 particles (diameter: 50-75 µm). After the blasting pre-treatment the disks were ultrasonically cleaned in Milli-Q water for 10 min at 30 °C and finally rinsed with acetone.

A coating solution containing 0.60 M Ru in 1-propanol was prepared by dissolving 7.450 g $RuCl_3 \times nH_2O$ (40.27 wt-% Ru, Heraeus) to a final volume of 50 ml in 1-propanol (Fischer Scientific). 100 µl of the coating solution was applied to cover the Ni surface and left for 2.5 min. A uniform distribution of coating solution over the Ni substrate was then obtained through a spin coater from Micro Systems Ltd for 30 s with a rotation speed of 4500 rpm. The electrodes were then left to dry in air for 5 min, followed by additional 5 min at 80 °C. Thermal decomposition of $RuCl_3$ to RuO_2 was performed at 500 °C for 12 min. The solution application, drying and calcination procedure was repeated until four layers of RuO_2 were deposited on each Ni disk. The heat treatment at 500 °C was prolonged to be one hour during the last coating cycle. With this method, RuO_2-coated Ni electrodes were obtained with a final metal loading of 4.54±0.17 g Ru m^{-2}. Prior to each electrochemical measurement, the electrode was cut to a size of 3.1 cm^2 and attached to a conductor; a 25 cm long Ni rod (diam. 1.5 mm) welded to the top end of the electrode.

2.2. Electrode characterization

The microstructure of the coating surfaces was studied using a LEO 1550 SEM and a SIGMA HV FEG-SEM, both systems from Zeiss, operated at 20 kV accelerator voltages. The latter was used to acquire high-resolution images of the electrode surface. A Versa 3D DualBeam microscope from FEI was used for cross-section images. Prior to ion beam milling, platinum was deposited on the electrode surface.

The electrochemical experiments required that a current feeder had to be welded on top of each RuO_2-coated Ni electrode. When the current feeders were removed after the electrochemical tests the top of the electrodes were slightly damaged, e.g. through removal of small part of the coating/substrate. Direct weight measurements, to determine the coating loss, were therefore not appropriate. Instead X-ray fluorescence measurements were performed

using the portable element analyzer NITON XLT898 from Thermo Scientific. The intensity of the Ru K_a peak was correlated to the coating amount obtained in mass Ru per area (g Ru m^{-2}) using six calibration samples with varying amount of coating layers of RuO_2 deposited on Ni substrates prepared using the spin coating technique as described earlier. For the calibration samples the amount of coating, in mass Ru per area, is determined through the actual weigh of the RuO_2 coating. An uncoated Ni disk was used as a blank. The Ru content of the electrodes was determined through the average of four XRF measurements at random selected spots before and after each electrochemical test using the calibration curve. Coating loss was calculated in weight-% Ru after each electrochemical test.

X-ray diffraction analysis was performed with an X´pert XRD system from Panalytical using Ni-filtered Cu K_α radiation. Symmetric θ-2θ scans were performed using normal Bragg-Brentano geometry. The sample preparation described in section 2.1 generates coatings that are built up by nanoparticles (see Fig. 1d) and the average particle size could be determined through the Scherrer equation [21,22] using the full width of half maximum (fwhm) and the shape factor K=0.9 for the RuO_2 (110) reflection.

2.3. Electrochemical measurements

The electrochemical measurements were performed in 8 M NaOH at 90.0±0.2 °C using an electrochemical cell with a three-electrode configuration where the RuO_2/Ni sample, a Ni-mesh, and a standard calomel electrode (sat. KCl) from Radiometer Copenhagen were used as a working electrode, a counter electrode, and a reference electrode, respectively. The working and counter electrodes were placed at a distance of forty mm from each other while the reference electrode was placed in an external compartment, which was connected via a tube to a Luggin capillary. The tip of the capillary was placed two mm from the surface of the working electrode to minimize the effect from the IR-drop in the electrolyte, but not too close to disturb the current distribution. No further IR-correction was used during the experiments. The electrochemical cell was prepared with a newly made sample and filled with fresh electrolyte prior to each electrochemical test. The electrolyte was prepared from NaOH pellets (reagent analytical grade, Scharlau) dissolved in Milli-Q water and was stirred continuously during each experiment. Although NaOH of analytical grade was used, impurities in the NaOH pellets (mainly Pb and Fe) were released into the electrolyte and some of it was deposited on the electrode surface during cathodic polarization. However, reducing the amount of impurities did not have any influence on the corrosion process during polarity

inversion. Analytical grade NaOH pellets, without additional purification, were therefore used for the electrochemical experiments presented in this report. Other possible sources of relevant impurities were scrutinized and the amounts of impurities were, thus, reduced to insignificant levels.

The deterioration of the RuO_2 coating was studied after different electrochemical treatments. Galvanostatic polarization was applied to produce hydrogen or oxygen gas at -6.4 and +6.4 kA m^{-2}, respectively. A polarity inversion test was used to simulate the effect of reverse currents during power shutdowns [4]. The current density was then cycled between cathodic (-6.4 kA m^{-2}, 30 min) and anodic (+6.4 kA m^{-2}, 30 min) polarization for six hours.

Cyclic voltammetry was performed with five repetitive scans between -1.2 to +0.5 V vs. SCE, immediately after cathodic (-6.4 kA m^{-2}, 2 h) or anodic (+6.4 kA m^{-2}, 2h) polarization. The scan rate was set to 20 mV/s. All electrochemical measurements were performed with an SI 2187 Electrochemical Interface potentiostat from Solartron Analytical.

2.4 Ultraviolet (UV) absorption spectrophotometry

UV-VIS absorption spectrophotometry was performed in the 350-600 nm wavelength range using an UV-1800 Shimadzu spectrophotometer.

3. Results and discussion

3.1. Morphological structure of RuO_2/Ni coatings

Fig. 1 shows a typical example of a spin coated disk electrode (diameter 25 mm) with RuO_2 deposited on a Ni substrate. The coating appears rather compact on a microscale and lacks the mud-cracked pattern usually obtained by other coating solution application techniques like brushing, spraying, or dipping [19] (Fig. 1b). Nevertheless, the coating is porous on a nanoscale and contains of small RuO_2 nanoparticles with a size of roughly 15-20 nm as shown in the high-resolution SEM (Fig. 1d). The average size of the RuO_2 nanoparticles is confirmed to be around 15 nm, as determined through the Scherrer equation applied on the RuO_2 (110) reflection.

Blasting pre-treatment is crucial to obtain acceptable adhesion strength of the RuO_2 coating to the Ni substrate. The disadvantage is, however, a rough coating surface with peaks and valleys (Fig. 1b), where thicker coating is obtained in the valleys compared to the peaks (Fig. 1c). The cross-section SEM image shows that the coating in the study varies from 0.4 to 1.4 µm at the thinnest and thickest regions, respectively. Still, the spin coating technique employed in this study generates a reproducible coating amount of 4.54 ±0.17 g Ru m^{-2}.

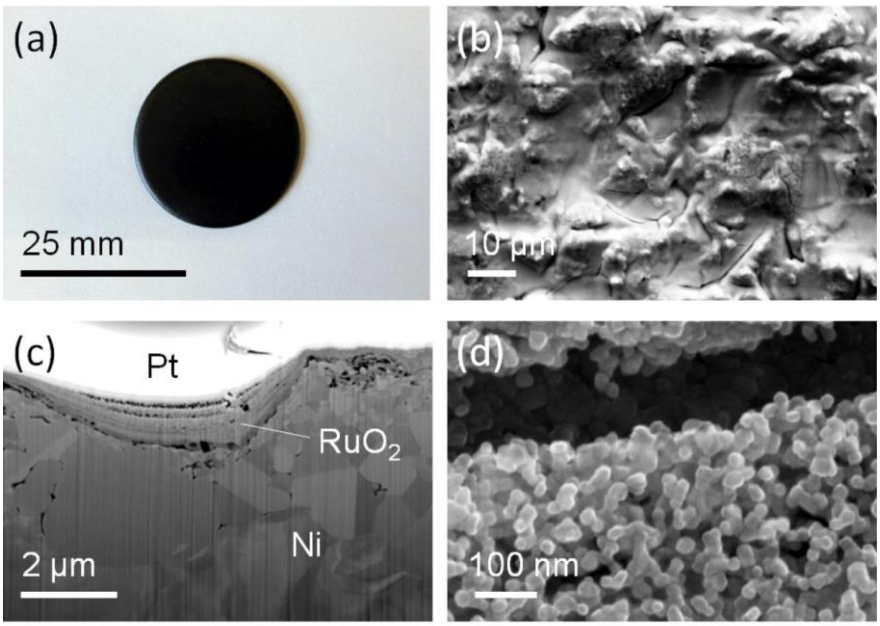

Fig. 1. RuO_2-coated nickel disk electrode at different length scales: (a) on a mm-scale, (b) on a microscale, (c) a cross-section of the coating, and (d) nanostructure of RuO_2 particles. The cross-section image was obtained after Pt deposition on the electrode surface followed by ion beam milling.

3.2. Effect of HER, OER, and reverse currents

Figure 2-3 present losses of coatings, measured with XRF and illustrated through SEM, respectively, as examples of the effect of the different electrochemical treatments performed in 8 M NaOH at 90 °C. Only small coating losses (<10 wt-% Ru) were obtained after plain anodic or cathodic polarization (0.5-6 hours). The coating loss is an effect from mechanical erosion caused by strong gas evolution, which introduces small cracks in the coating structure and, as seen in Fig. 3b, even causes loss of coating fragments as flakes from the top layer. On the other hand, when polarity inversion was introduced immediately after the hydrogen evolution the samples show extensive loss of coating material. Fig. 2 show that about 50 wt-% of the RuO_2 coating was lost when the current density was cycled between the cathodic and anodic region using the polarity inversion test as described in the Experimental Section.

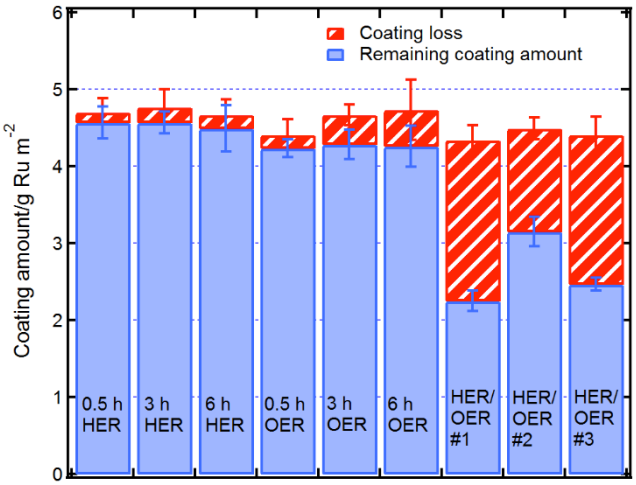

Fig. 2. Example of coating losses measured with XRF for spin coated RuO_2/Ni electrodes subjected to 0.5-6 h HER (-6.4 kA m^{-2}), 0.5-6 h OER (+6.4 kA m^{-2}) and reverse currents in different cycled polarity inversion tests (HER/OER). HER/OER#1: the electrode was cycled between -6.4 and +6.4 kA m^{-2} in a polarity inversion test, HER/OER#2: the electrode was cycled between -6.4 kA m^{-2} and 0.0026 kA m^{-2}. 1, HER/OER#3: the electrode was cycled between -6.4 and +6.4 kA m^{-2}, but interrupted after 3.5 cycles and, thus, ending the test with a cathodic step in the polarity inversion test. Electrolyte: 8 M NaOH at 90 °C. The error bars show the standard deviation from four measurements at random selected spots on each sample.

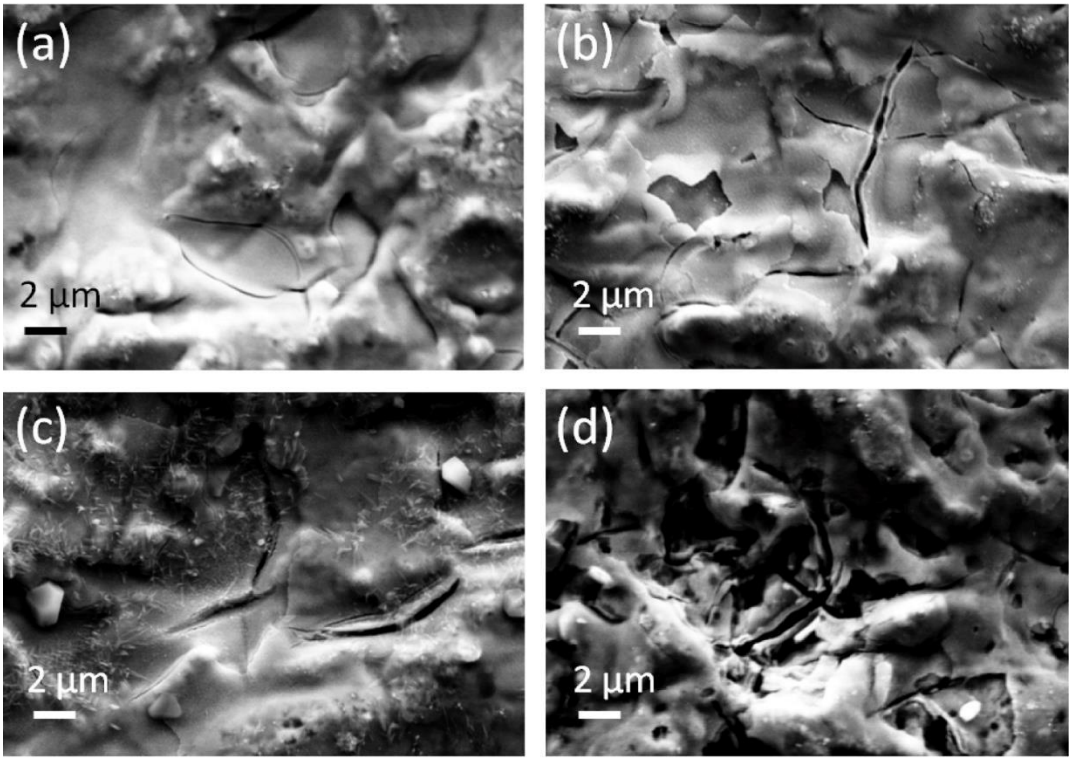

Fig. 3. SEM images for spin coated RuO_2/Ni electrodes subjected to different electrochemical tests: (a) a pristine coating, (b) after 6 h OER (+6.4 kA m^{-2}), (c) after 6 h HER (-6.4 kA m^{-2}), and (d) after a cycled polarity inversion test.. Electrolyte: 8 M NaOH at 90 °C.

Cyclic voltammetry revealed that different corrosion processes occurred depending on the previously applied electrochemical treatment (cathodic or anodic polarization). The applied potential was cycled five times between -1.2 and +0.5 V vs. SCE, i.e. between the hydrogen and oxygen evolution reaction, respectively, as shown in Fig. 4. The most noticeable is the first scan of the sample exposed to extensive hydrogen evolution. A large oxidation peak appears at about -1.05 V vs. SCE caused by re-oxidation of hydrogen gas trapped inside the nanoporous coating structure [6,23]. More important is, however, the oxidation peak at about +0.15 V vs. SCE indicating oxidation of Ru^{4+} to Ru^{6+}, which suggests formation of ruthenate ions, RuO_4^{2-} [6,24,25]. The RuO_4^{2-} formation is also observed in the first cycle of the reference sample, which is a consequence of that the cyclic voltammetry starts on the HER side. This is not the case after extensive oxygen evolution.

Furthermore, it is obvious that the RuO_2 coating also contains Ni in some form as the oxidation peak for Ni^{2+}/Ni^{3+} at about + 0.30 V vs. SCE is observed in the cyclic voltammetry of all three samples and, in addition, the Ni^0/Ni^{2+} peak at -0.85 V in the first scan of the HER

(2 h) sample [6,26,27]. Nickel content in RuO_2 coatings applied on Ni substrates has been confirmed with XPS [18]. The study showed that a RuO_2 coating of a newly made electrode has a substantial amount of nickel oxide (NiO), which after exposure to hydrogen evolution transforms into $Ni(OH)_2$ and metallic Ni. The Ni^{2+}/Ni^{3+} peak in cyclic voltammetry shown in Fig. 4 can therefore be associated with the transformation from NiO to nickel oxyhydroxide (NiOOH). When the potential is scanned in the reverse direction, a corresponding Ni^{3+}/Ni^{2+} reduction peak appears at about +0.10 V vs. SCE. The presence of the Ni^{0}/Ni^{2+} peak in the HER (2 h) sample supports the XPS study showing that NiO is reduced to metallic Ni during extensive hydrogen evolution. Although present in the RuO_2 coating, we have confirmed that different amount of Ni in the RuO_2 coating does not significantly influence on the corrosion process of the RuO_2 coating.

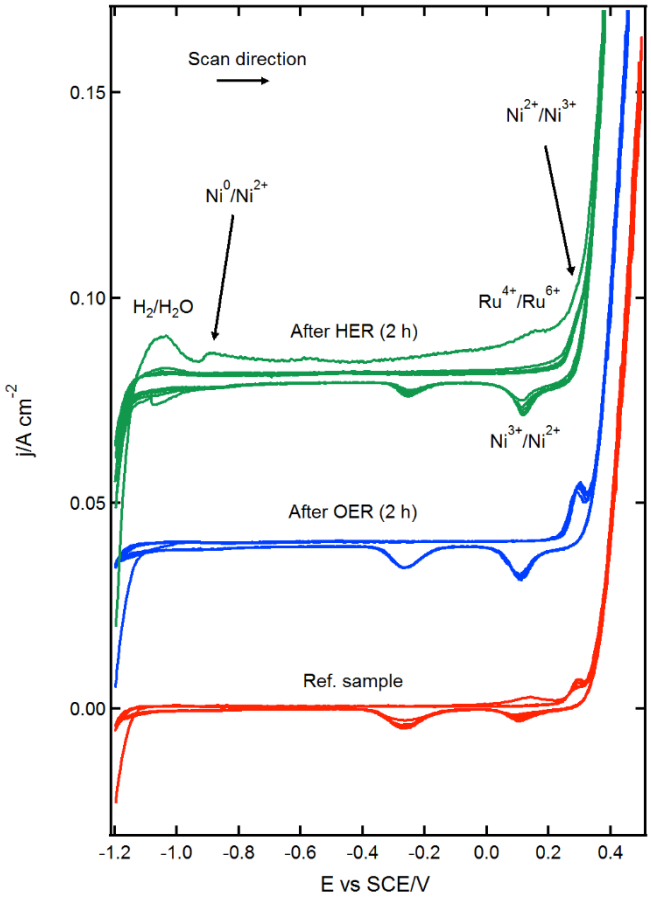

Fig. 4. Cyclic voltammetry measured for RuO_2/Ni electrodes subjected to either OER (+6.4 kA m^{-2}) or HER (-6.4 kA m^{-2}) for two hours in 8 M NaOH at 90 °C. A voltammogram for a reference RuO_2/Ni electrode is included for comparison. For clarity the curves for the OER and HER samples are offset by 0.4 and 0.8 A/cm^2, respectively.

A reduction peak at about -0.25 V vs. SCE appears in the reverse scan direction in all three cyclic voltammograms. This peak is suggested to be the reduction of peroxide ions produced during extensive oxygen evolution [23,28] and is therefore not related to corrosion of the electrode material.

Figure 5, which shows a UV-VIS spectrophotogram of the electrolyte from a polarity inversion test, confirms the formation of RuO_4^{2-} as the electrode was cycled [29,30]. In addition to the absorption peak at 465 nm the electrolyte had the characteristic yellow-brown discoloring developed during the cycled polarity inversion test, which was not the case when plain cathodic or anodic polarization was applied. Although not observed in the cyclic voltammogram in Fig. 4, it is possible that ruthenium species with higher oxidation states (Ru^{7+}, Ru^{8+} etc.) also were obtained during the corrosion process [14,25], but those peaks would be masked in the region for oxidation of Ni^{2+} to Ni^{3+} and the oxygen evolution reaction.

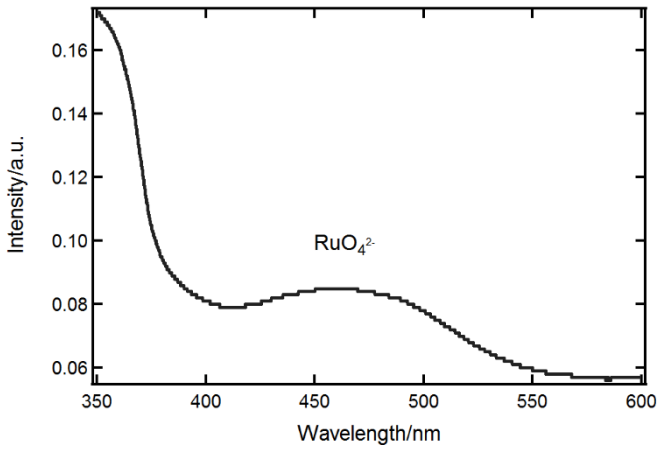

Fig. 5. UV-VIS spectrophotometry performed on the electrolyte (8M NaOH at 90 °C) after a polarity inversion test. The absorption peak found at 465 nm is typical for ruthenate ions (RuO_4^{2-}) [25,29,30].

The effect of HER, OER, and reverse currents on the crystal phases of RuO_2 was studied through XRD and obtained diffractograms are presented in Fig. 6. The main rutile peaks for a fresh sample of a RuO_2 coating appear at 27.9, 35.1, 39.8, 54.2, and 57.6 degrees. Additional peaks originate from the substrate and appear as Ni at 44.5, 51.8, and 76.4 degrees and NiO at 37.2, 43.3, and 62.9 degrees. At 25.6 degrees there is a small peak that we assign to Al_2O_3, which is derived from particles of blasting material incorporated in the Ni surface. A typical

diffractogram for a RuO_2 coating after OER shows no deviation compared to a pristine sample. A diffractogram for a RuO_2 coating after HER shows, on the other hand, a substantial change in crystallinity. With increasing duration of the cathodic polarization the rutile 110 peak at 27.9 degrees, enlarged in Fig. 7(a), reduces significantly. Simultaneously there is a growth of a new peak at 26.5 degrees. The corresponding anodic polarization test does not induce any changes of the rutile 110 peak, as shown in Fig. 7(b). This observation suggests that a phase transformation occurs during extensive hydrogen evolution. The peak at 26.5 degrees has been observed before [3,11], although never discussed in detail. It was, however, speculated that this peak originates from hydrated RuO_2 or possibly hydroxylated Ru-species formed during strong hydrogen evolution in alkaline medium. Recently, we were able to determine this phase to be more specifically $RuO(OH)_2$ [18]. The diffractogram of the RuO_2 coating that has been exposed to the polarity inversion test shows, on the other hand, no peak at 26.5 degrees indicating that the hydroxylated phase, formed during extensive hydrogen evolution, is removed during extensive oxygen evolution, see Fig. 7c. In addition, the rutile 110 peak at 27.9 degrees is not only smaller but also broader indicating that the RuO_2 coating consists of particles with smaller crystallite size compared to a pristine sample of RuO_2. For example, when HER was applied for six hours followed by OER for six hours, the average diameter of the RuO_2 particles decreased from 15.1±0.2 to 13.6±0.4 nm, i.e. a size reduction of 10 %.

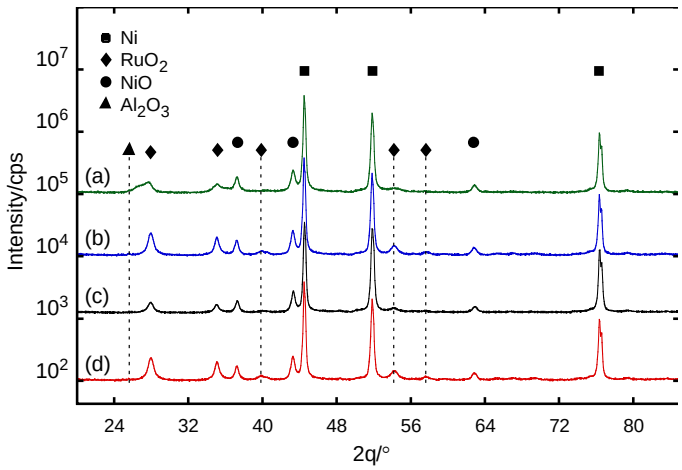

Fig. 6. θ-2θ XRD diffractograms from RuO_2/Ni electrodes after (a) HER (-6.4 kA m^{-2}) 6 h, (b) OER (+6.4 kA m^{-2}) 6 h, and (c) HER (-6.4 kA m^{-2}) 6 h + OER (+6.4 kA m^{-2}) 6 h compared to (d) a pristine RuO_2-coating.

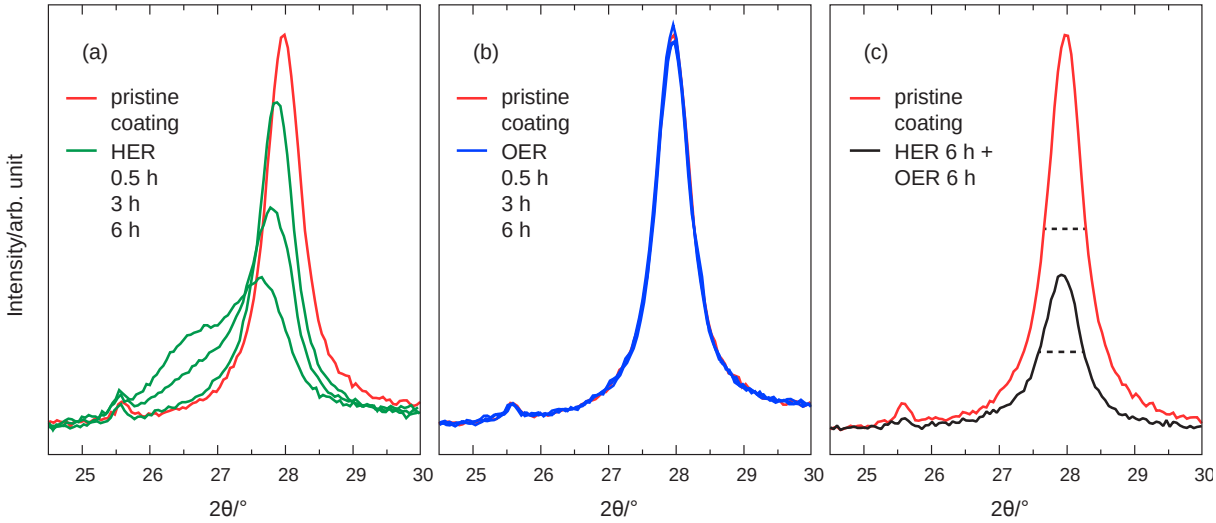

Fig. 7. Rutile 110 peak for RuO_2/Ni electrode after (a) HER 0.5, 3, and 6 h, (b) OER 0.5, 3, and 6 h, and (c) HER 6 h + OER 6 h; the current densities were -6.4 kA m^{-2} and +6.4 kA m^{-2} for HER and OER, respectively. A rutile 110 peak from a pristine coating is included as a reference in all three panels. In (c) the fwhm (dashed line) increases from 0.62±0.01 to 0.68±0.02 degrees suggesting a reduced particle size after the electrochemical treatment.

3.3. Effect of anodic currents densities on coating loss in polarity inversion test

In industrial applications the size of the reverse currents obtained during power shutdowns, e.g. in alkaline water electrolysis, is usually smaller (<0.1 kA m^{-2}) than the anodic currents that we have adopted in the polarity inversion test described in the Experimental section. It is therefore relevant to investigate the effect of the applied anodic current density on the coating loss. Fig. 8 shows the result from a cycled polarity inversion test where the cathodic current density was -6.4 kA m^{-2} while the anodic current density was increased from $6{,}4\times10^{-4}$ to 6,4 kA m^{-2} for each individual electrodes. The test shows that the electrochemical corrosion starts at relatively low anodic current densities, more specifically at a threshold value of about $2.5\text{x}10^{-3}$ kA m^{-2}. When the applied anodic current density was further increased by an order of magnitude the corrosion process leveled out, most likely because of the limited amount of $RuO(OH)_2$ produced during each cathodic step in the test. This implies that the corrosion process comes to an end when the hydroxylated phase is removed completely during the following anodic step. Once again, no hydroxylated phase could be found in the XRD diffractogram after the final anodic step in the polarity inversion test. However, if the polarity inversion test was stopped after 3.5 cycles, i.e. ending with a cathodic step, $RuO(OH)_2$ was present (data not shown).

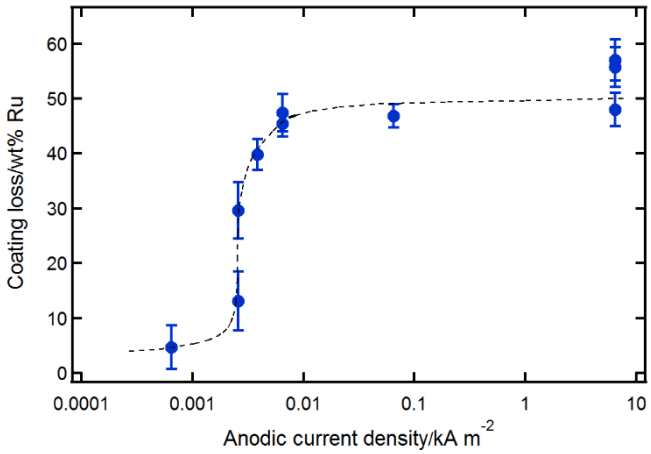

Fig. 8. Coating loss measured with XRF for individual RuO_2/Ni electrodes as an effect of anodic current density in a cycled polarity inversion test. Electrolyte: 8 M NaOH at 90 °C. The error bars represent standard deviation calculated from four XRF measurements at random selected spots on each sample, before and after each test.

3.4. Description of corrosion process

From the presented results we can illustrate the corrosion of RuO_2-based electrodes subjected to reverse currents in strong alkaline medium. Fig. 9 displays a simple sketch showing that during HER an essential part of the surface of the RuO_2 nanoparticles is transformed into hydroxylated Ru-species, which we recently have identified as $RuO(OH)_2$ [18]. When anodic currents are applied after the HER the hydroxylated Ru-species will electrochemically corrode to RuO_4^{2-}, and possibly higher oxidation states, that dissolves into the electrolyte leaving an electrode coating with smaller nanoparticles. The corrosion process ceases when all hydroxylated Ru-species are consumed in the anodic step. Further phase transformation followed by electrochemical corrosion will occur if cycling between cathodic and anodic polarization is repeated, resulting in smaller and smaller RuO_2 nanoparticles.

In real industrial applications much longer duration of cathodic polarization is expected before any interruption of the process occurs. It is then realistic to believe that the entire RuO_2 coating might be transformed into $RuO(OH)_2$ and the worst-case scenario might then be that the entire electrode coating will corrode when the cathode is subjected to reverse currents during unprotected conditions, e.g. no use of polarization rectifiers or poorly working rectifiers during power shutdowns. Other parameters that most likely will influence the rate of hydrogen absorption and formation of $RuO(OH)_2$ during HER, and subsequently the extent of

corrosion caused by reverse currents, are applied cathodic current density, electrolyte concentration, and temperature.

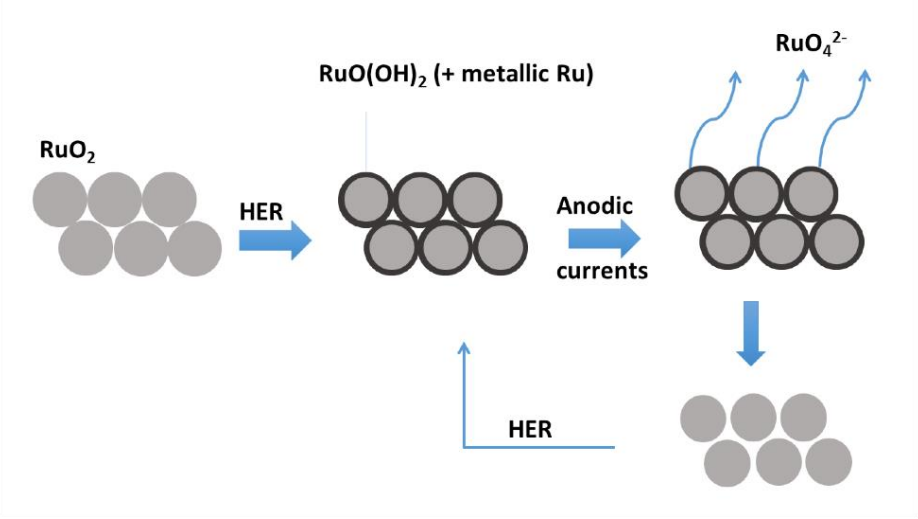

Fig. 9. Simple illustration of the corrosion of RuO_2 coatings subjected to polarity inversion after HER in alkaline medium. RuO_2 nanoparticles that are exposed to hydrogen evolution develop a shell of $RuO(OH)_2$ (and metallic Ru) [18]. Anodic polarization causes oxidation of $RuO(OH)_2$ into RuO_4^{2-} that dissolves into the electrolyte. The corrosion process comes to an end when all $RuO(OH)_2$ is oxidized and the remaining coating consists of RuO_2 with smaller nanoparticle sizes.

4. Conclusions

In this work we show why RuO_2-based coatings in strong alkaline environments are sensitive to reverse currents. Because of the extent of hydrogen exposure during cathodic polarization, a substantial amount of the RuO_2 coating is transformed into hydroxylated phases that are far more sensitive to revere currents compared to a RuO_2 coating subjected to only anodic polarization. When an anodic current is introduced after extensive hydrogen evolution the hydroxylated Ru-species oxidizes and form Ru^{6+} species and possibly compounds with even higher oxidation states. During the studied time scale, the corrosion process ceased as soon as all hydroxylated phase was consumed, leaving an electrode coating with smaller RuO_2 nanoparticles.

Acknowledgments

The Swedish Research Council (project nr. 2007-5059) is acknowledged for funding this study. The study has partly been accomplished through funding from the European Research Council under the European Communities Seventh Framework Program (FP7/2007-2013)/ERC Grant agreement no. [258509], the Swedish Research Council (VR) grant no. 642-2013-8020, and the KAW Fellowship program. Ellen Baken, FEI and Heiner Jaksch, Carl Zeiss NTS are highly acknowledged for providing the cross-section and high-resolution SEM images, respectively, and the assistance from Bernth Nordin, Permascand, with pre-treatment of some electrodes was very much appreciated. SH also thanks Joakim Bäckström, Håkan Olin and Torbjörn Carlberg from Mid-Sweden University, Ann Cornell, Rasmus Karlsson and Göran Lindbergh from KTH Royal Technical Institute, and Lars-Erik Bergman, Ingemar Johansson and John Gustavsson from Permascand for valuable discussions.

References

[1] T.F. O'Brien, T.V. Bommaraju, F. Hine, Handbook of chlor-alkali technology. Volume I: Fundamentals, Springer Science+Business Media, New York, 2005.

[2] T.F. O'Brien, T.V. Bommaraju, F. Hine, Handbook of chlor-alkali technology. Volume II: Brine treatment and cell-operation, Springer Science+Business Media, New York, 2005.

[3] C. Iwakura, M. Tanaka, S. Nakamatsu, H. Inoue, M. Matsuoka, N. Furukawa, Electrochemical properties of Ni/(Ni+RuO_2) active cathodes for hydrogen evolution in chlor-alkali electrolysis, Electrochim. Acta 40 (1995) 977.

[4] M.B.I. Janjua, R.L. Le Roy, Electrocatalyst performance in industrial water electrolysers, Int. J. Hydrogen Energy 10 (1985) 11.

[5] B. Børresen, G. Hagen, R. Tunold, Hydrogen evolution on $Ru_x\ Ti_{1-x}\ O_2$ in 0.5 M H_2SO_4, Electrochim. Acta 47 (2002) 1819.

[6] V.D. Jović, U. Lačnjevac, B.M. Jović, N.V. Krstajić, Service life test of non-noble metal composite cathodes for hydrogen evolution in sodium hydroxide solution, Electrochim. Acta 63 (2012) 124.

[7] S. Ardizzone, G. Fregonara, S. Trasatti, Influence of hydrogen evolution on the voltammetric charge of RuO_2 electrodes, J. Electroanal. Chem. 266 (1989) 191.

[8] M. Blouin, D. Guay, Activation of ruthenium dioxide, iridium dioxide, and mixed Ru_xIr_{1-x} oxide electrodes during cathodic polarization and hydrogen evolution, J. Electrochem. Soc. 144 (1997) 573.

[9] L.D. Burke, N.S. Naser, Metastability and electrocatalytic activity of ruthenium dioxide cathodes used in water electrolysis cells, J. Appl. Electrochem. 35 (2005) 931.

[10] C. Chabanier, D. Guay, Activation and hydrogen absorption in thermally prepared RuO_2 and IrO_2, J. Electroanal. Chem. 570 (2004) 13.

[11] T. Hachiya, T. Sasaki, K. Tsuchida, H. Houda, Ruthenium oxide cathodes for chlor-alkali electrolysis, ECS Trans. 16 (2009) 31.

[12] L. Chen, D. Guay, F.H. Pollak, F. Lévy, AFM observation of surface activation of ruthenium oxide electrodes during hydrogen evolution, J. Electroanal. Chem. 429 (1997) 185.

[13] A. Cornell, D. Simonsson, ruthenium dioxide as cathode material for hydrogen evolution in hydroxide and chlorate solutions, J. Electrochem. Soc. 140 (1993) 3123.

[14] M. Pourbaix, Atlas of electrochemical equilibria in aqueous solutions (Engl. Ed.), Pergamon press, Oxford, 1966.

[15] N. Takeno, Atlas of Eh-pH diagrams; Intercomparison of thermodynamic databases, Geological Survey of Japan Open File Report No. 419, 2005.

[16] E.R. Kötz, J. Stucki, Ruthenium dioxide as a hydrogen-evolving cathode, J. Appl. Electrochem. 17 (1987) 1190.

[17] D. Rochefort, P. Dabo, D. Guay, P.M.A. Sherwood, XPS investigations of thermally prepared RuO_2 electrodes in reductive conditions, Electrochim. Acta 48 (2003) 4245.

[18] L.-Å. Näslund, Á.S. Ingason, S. Holmin, R. Rosen, Formation of $RuO(OH)_2$ on RuO_2-based electrodes for hydrogen production, J. Phys. Chem. C. 118 (2014) 15315.

[19] P. Shrivastava, M.S. Moats, Wet film application techniques and their effects on the stability of RuO_2–TiO_2 coated titanium anodes, J. Appl. Electrochem. 39 (2009) 107.

[20] C. Hummelgård, J. Gustavsson, A. Cornell, H. Olin, J. Bäckström, Spin coated titanium–ruthenium oxide thin films, Thin Solid Films 536 (2013) 74.

[21] H.P. Klug, L.-E. Alexander, X-ray diffraction procedures: for polycrystalline and amorphous materials, 2nd ed. Wiley, New York, 1974.

[22] C. Malmgren, A.K. Eriksson, A. Cornell, J. Bäckström, S. Eriksson, H. Olin, Nanocrystallinity in RuO_2 coatings-influence of precursor and preparation temperature, Thin Solid Films 518 (2010) 3615.

[23] L. Roué, D. Guay, R. Schulz, Hydrogen electrosorption in nanocrystalline Ti-based alloys, J. Electroanal. Chem. Interfacial. Electrochem. 480 (2000) 64.

[24] L.D. Burke, O.J. Murphy, The electrochemical behaviour of RuO_2-based metal oxide anodes in base, J. Electroanal. Chem. 109 (1980) 199.

[25] J. Juodkazytė, R. Vilkauskaitė, B. Šebeka, K. Juodkazis, Difference between surface electrochemistry of ruthenium and RuO_2 electrodes, Trans. Inst. Met. Finish. 85 (2007) 194.

[26] M.A. Domínguez-Crespo, A.M. Torres-Huerta, B. Brachetti-Sibaja, A. Flores-Vela, Electrochemical performance of Ni-RE (RE=rare earth) as electrode material for hydrogen evolution in alkaline medium, Int. J. Hydrogen Energy 36 (2011) 135.

[27] M.E.G. Lyons, L. Russell, M. O´Brien, R.L. Doyle, I. Godwin, M.P. Brandon, Redox switching and oxygen evolution at hydrous oxyhydroxide modified nickel electrodes in aqueous alkaline solution: effect of hydrous oxide thickness and base concentration, Int. J. Electrochem. Sci. 7 (2012) 2710.

[28] W. O´Grady, C. Iwakura, J. Huang, E. Yeager, Ruthenium oxide catalysts for the oxygen electrode, in: M.W. Breiter (Ed.), Proceedings of the Symposium on Electrocatalysis, Princeton, 1974, p. 286.

[29] R.E. Connick, C.R. Hurley, Chemistry of Ru(VI), -(VII) and –(VIII), Reactions, oxidation potentials and spectra, J. Am. Chem. Soc. 74 (1952) 5012.

[30] L. Roué, D. Guay, R. Schulz, Electrochemical behavior of nanocrystalline Ti_2RuFe alloy prepared by high energy ball-milling, J. Electroanal. Chem. 455 (1998) 83.